This article was downloaded by:
On: *15 January 2011*
Access details: *Access Details: Free Access*
Publisher *Taylor & Francis*
Informa Ltd Registered in England and Wales Registered Number: 1072954 Registered office: Mortimer House, 37-41 Mortimer Street, London W1T 3JH, UK

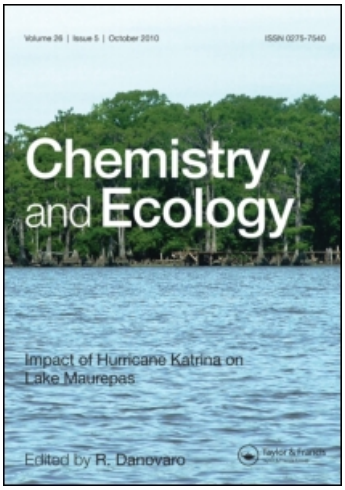

Chemistry and Ecology
Publication details, including instructions for authors and subscription information:
http://www.informaworld.com/smpp/title~content=t713455114

Water circulation and transport timescales in the Gulf of Oristano

Andrea Cucco[a]; Angelo Perilli[a]; Gianni De Falco[b]; Michol Ghezzo[a]; Georg Umgiesser[c]
[a] Istituto Ambiente Marino Costiero, IAMC-CNR, sezione di Oristano, c/o IMC—International Marine Centre, Localita Sa Mardini, Oristano, Italy [b] International Marine Centre, IMC, Localita Sa Mardini, Oristano, Italy [c] Istituto di Scienze Marine, ISMAR-CNR, Italy

To cite this Article Cucco, Andrea , Perilli, Angelo , De Falco, Gianni , Ghezzo, Michol and Umgiesser, Georg(2006) 'Water circulation and transport timescales in the Gulf of Oristano', Chemistry and Ecology, 22: 4, S307 — S331
To link to this Article: DOI: 10.1080/02757540600670364
URL: http://dx.doi.org/10.1080/02757540600670364

PLEASE SCROLL DOWN FOR ARTICLE

Full terms and conditions of use: http://www.informaworld.com/terms-and-conditions-of-access.pdf

This article may be used for research, teaching and private study purposes. Any substantial or systematic reproduction, re-distribution, re-selling, loan or sub-licensing, systematic supply or distribution in any form to anyone is expressly forbidden.

The publisher does not give any warranty express or implied or make any representation that the contents will be complete or accurate or up to date. The accuracy of any instructions, formulae and drug doses should be independently verified with primary sources. The publisher shall not be liable for any loss, actions, claims, proceedings, demand or costs or damages whatsoever or howsoever caused arising directly or indirectly in connection with or arising out of the use of this material.

Chemistry and Ecology
August 2006, Vol. 22 (Supplement 1), pp. S307–S331

Taylor & Francis
Taylor & Francis Group

Water circulation and transport timescales in the Gulf of Oristano

ANDREA CUCCO*†, ANGELO PERILLI†, GIANNI DE FALCO‡, MICHOL GHEZZO† and GEORG UMGIESSER§

†Istituto Ambiente Marino Costiero, IAMC-CNR, sezione di Oristano, c/o IMC—International Marine Centre, Localita Sa Mardini, Oristano, Italy
‡International Marine Centre, IMC, Localita Sa Mardini, Oristano, Italy
§Istituto di Scienze Marine, ISMAR-CNR, S. Polo 1364, 30125 Venice, Italy

(Received 2 March 2005; in final form 24 February 2006)

Downloaded At: 12:58 15 January 2011

In this work, water circulation in the Gulf of Oristano was investigated using a 2D hydrodynamic model. The model is based on the finite-element method. This solves the shallow-water equations on a spatial domain representing the Gulf of Oristano and the surrounding coastal sea. The hydrodynamic features of the gulf were investigated when the basin is influenced by different wind regimes. In order to evaluate the renewal capacity of the basin, the residence and the transit times were computed for each scenario. The study reveals that the gulf is characterized by circulation patterns promoting strong trapping phenomena. The results obtained are partially confirmed by the heavy-metal distribution in the sediments. In particular, the southern part of the basin is characterized by the presence of high heavy-metal concentrations in the bottom sediment, in the same areas where model results reveal a strong trapping capacity. This study can be considered as a first attempt to investigate the wind-driven water circulation in the Gulf of Oristano, and the results obtained can help in planning hydrological campaigns in the basin.

Keywords: Water circulation; Transport; Timescale; Gulf of Oristano

1. Introduction

The Gulf of Oristano (see figure 1) is a semi-enclosed embayment on the western coast of the Sardinia island (Italy: latitude 39°50′; longitude 8°30′). It is a shallow water basin with an average depth of about 15 m and a maximum depth of about 25 m. It covers an area of 150 km^2 and is connected to the Sardinian Sea through an opening 9 km length between the San Marco cape at the north and Frasca cape at the south.

The surrounding mainland is characterized by the presence of lagoon and salt-marsh systems connected to the gulf through artificial narrow channels. In particular, a large lagoon system, the Cabras lagoon, discharges its water through an inlet (the Scolmatore channel) located in the northern part of the gulf. Along the eastern border of the basin, the Tirso river mouth is

*Corresponding author. Email: andrea.cucco@iamc.cnr.it

Chemistry and Ecology
ISSN 0275-7540 print/ISSN 1029-0370 online © 2006 Taylor & Francis
http://www.tandf.co.uk/journals
DOI: 10.1080/02757540600670364

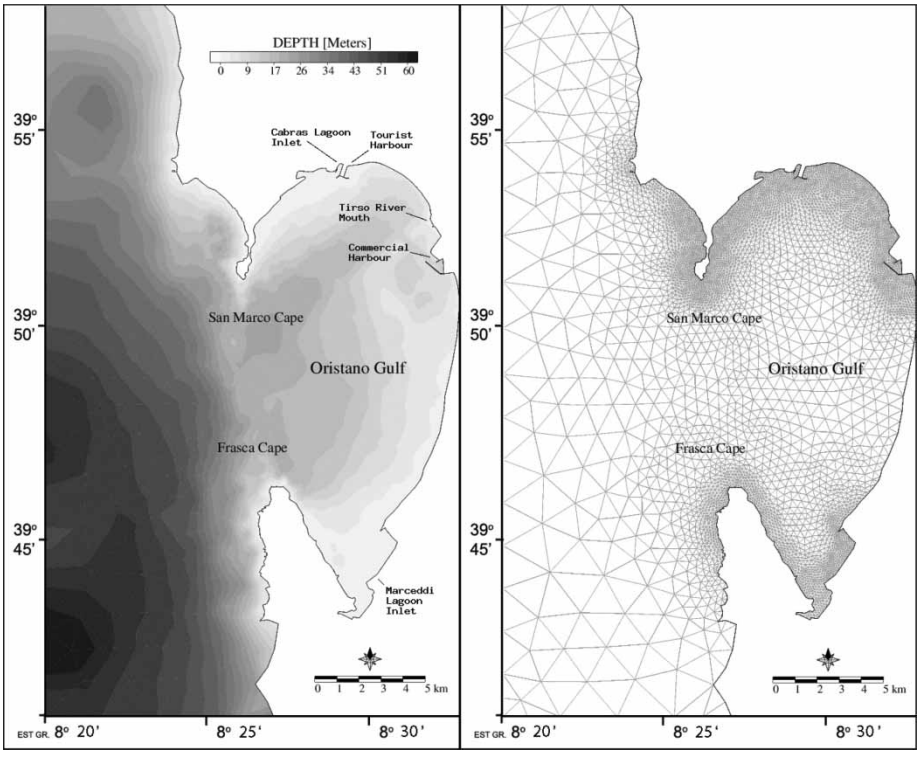

Figure 1. Bathymetry and finite-element grid of the Oristano Gulf. The gulf and sea are connected through a large opening, about 9 km length, between the San Marco cape (north) and the Frasca cape (south).

Downloaded At: 12:58 15 January 2011

located between a touristic harbour (at the north) and an industrial harbour (at the south). In the northern part of the basin, between the San Marco cape and the eastern gulf border, there is a deep navigable channel with an average depth of about 15 m, connecting the industrial harbour to the open sea. A further wide lagoon system, the Marceddì and S. Giovanni lagoons, discharges water into the gulf through an inlet located in the southern part of the basin. The lagoons are exploited by intense fishery and aquaculture activities and collect the sewage-treatment-plant discharges from the surrounding cities (Oristano and Cabras) into the gulf.

The typical wind regimes are the Mistral from north-west (NW), the Libeccio from the south-west (SW) and the Sirocco from the south-east (SE). The Mistral can be considered as the main meteorological forcing. The yearly average wind speed is about $10\,\mathrm{m\,s^{-1}}$ for the Mistral regime, $9\,\mathrm{m\,s^{-1}}$ for the Libeccio regime, and $10\,\mathrm{m\,s^{-1}}$ for the Sirocco regime [1].

The long-scale offshore circulation is mainly characterized by anticyclonic gyres generated by the baroclinic instabilities of the Algerian Current system. The main assumption is that these dynamics do not influence the water circulation inside the gulf and the surrounding areas. This consideration is supported by the shallowness of the embayment and by the presence of a spread shelf area with a depth lower than 100 m off the Oristano Gulf. Both numerical simulations of the water circulation in the Sardinia Sea and hydrographical measurements reveal the presence of two anticyclonic gyres located about 200 km off the west coast of Sardinia Island. The influence of these structures on the water circulation inside the gulf is then negligible due to their distance from the coast.

The astronomic tides in the area are very weak, and the maximum water displacement measured in the gulf in the absence of wind is about 20 cm (±10 cm) [2]. Therefore, the tidal-induced water circulation can be neglected especially when strong wind events occur in the area.

The freshwater inputs in the gulf are characterized by a torrent-like regime with flows close to zero in summer when the rainfall is poor. Nevertheless, during the winter period, when precipitations are abundant, the flows of the rivers and channels discharging into the gulf and in the surrounding lagoons are very low. This is due to the presence of many artificial basins and dams, which strongly reduce the drainage of the rainfall in the catchment area. In particular, the average discharge of the Tirso river, that is the only freshwater input flowing directly into the gulf, is lower than 5 $m^3 s^{-1}$, a value that is too low to promote any remarkable baroclinic-induced water circulation [3].

Concerning the Cabras lagoon, the water exchanges with the gulf are governed by the tides. The water masses flow through the Lagoon inlet with an average discharge lower than 20 $m^3 s^{-1}$. The salinity of the water masses flowing out through the inlet during the ebb tide, is strictly related to the intensity of the tidal mixing and to the amount of the freshwater inputs flowing into the lagoon. With the tidal currents being very weak and the freshwater inputs very low compared with the average volume of the Cabras lagoon [2], the salinity gradients outside the inlet cannot be so sharp to generate any appreciable density-induced currents. Therefore, from the previous considerations, the wind can be considered as the main force for water circulation inside the Gulf of Oristano.

Downloaded At: 12:58 15 January 2011

The northern cape of the gulf, the San Marco cape, and the surrounding coastal zone constitute a marine protected area where anthropic activities, such as fishery and aquaculture, are forbidden. Even if this area is well protected by the direct exploitation of its resources, the maintenance of its ecological status is threatened by the impact of anthropic inputs produced by aquaculture activities taking place especially in the Cabras and Marceddì lagoons. A fundamental role on the transport of the produced pollutants and on the risk of contamination inside the gulf is given by the water circulation.

In this work, the wind-driven circulation inside the Gulf of Oristano was investigated by means of numerical modelling. The wind-induced water circulation was analysed under different meteorological forcings. In particular, the three typical wind regimes were considered as forcing scenarios. Moreover, the transport timescale of the basin was analysed for each forcing condition with the aim of correlating the basin renewal features with the concentrations of heavy metals in the bottom sediment.

The Oristano Gulf has never been subject to intense field measurements, especially from a hydrological stand point. The deficiency of experimental data that would be needed to characterize the hydrodynamics features of the gulf can strongly disturb any numerical application that investigates the water circulation in the basin.

Nevertheless, even with these limitations, this study has to be considered as a valid and realistic preliminary attempt to reproduce the hydrodynamic features of the Oristano Gulf. In particular, the results obtained, giving a first sketch of the circulation patterns in the embayment, represent a fundamental base for planning future measurement campaigns to collect hydrological data to further corroborate the model results.

2. Methods

In this section, the adopted numerical models and the two techniques used to compute the basin transport timescale are described. Furthermore, the methods followed for the geochemical analysis of the bottom sediments are reported.

2.1 *Hydrodynamic model*

A 2D hydrodynamic model of the Oristano Gulf, based on the finite-element method, was used [4–7]. The model was applied successfully in other previous studies with the aim of investigating both the hydrodynamics and the flushing features of lagoon and coastal basin systems [4–7].

The numerical computation was carried out on a spatial domain that represents the Gulf of Oristano through a finite-element grid. The grid contains 12,312 nodes and 18,987 triangular elements (see figure 1).

The model considers the open sea borders of the domain as open boundaries, and elsewhere the whole perimeter of the basin as closed boundaries. Finite elements are used for spatial integration, and a semi-implicit algorithm is adopted for the time integration. The terms treated implicitly are the water-level gradients and the Coriolis terms in the momentum equation and the divergence term in the continuity equation. The friction term is treated implicitly; all other terms are treated explicitly. The model resolves the vertically integrated shallow water equations in their formulations with water levels and transports:

$$\frac{\partial U}{\partial t} - fV + gH\frac{\partial \zeta}{\partial \chi} + RU + X = 0 \tag{1}$$

$$\frac{\partial V}{\partial t} + fU + gH\frac{\partial \zeta}{\partial y} + RV + Y = 0 \tag{2}$$

$$\frac{\partial \zeta}{\partial t} + \frac{\partial U}{\partial \chi} + \frac{\partial V}{\partial y} = 0, \tag{3}$$

where ζ is the water level, U and V the vertically integrated velocities (total or barotropic transports) in the x and y direction, g the gravitational acceleration, $H = h + \zeta$ the total water depth, h the undisturbed water depth, t the time, R the friction parameter, and f the Coriolis term. The terms X and Y contain all other terms like the wind stress, the nonlinear advective terms, and those that do not need to be treated implicitly in the time discretization. The wind stress is computed with the following formula:

$$\tau^x = \frac{\rho_a}{\rho_0} C_D |u| u^x \quad \tau^y = \frac{\rho_a}{\rho_0} C_D |u| u^y, \tag{4}$$

where ρ_a and ρ_0 denote the density of air and water, respectively, u the modulus of wind speed and u^x and u^y the components of wind speed in the x and y direction. In this formulation, C_D is a dimensionless drag coefficient that varies between 1.5×10^{-3} and 3.2×10^{-3}. The friction term was expressed as:

$$R = \frac{g\sqrt{u^2 + v^2}}{CH},$$

where C is the Chezy coefficient, which varies with the water depth as:

$$C = k_S H^{16},$$

where k_S is the Strickler coefficient. Details of the numerical treatment are given in Umgiesser and Bergamasco [5] and Umgiesser *et al.* [6].

At the open boundary, the water levels can be prescribed in accordance with the Dirichlet condition, and the water transports are computed by the model, in accordance with a radiative condition. At the closed boundaries, only the normal velocity is set to zero, and the tangential velocity is a free parameter. This corresponds to a full slip condition.

Downloaded At: 12:58 15 January 2011

Downloaded At: 12:58 15 January 2011

2.2 *Transport timescales*

Flushing features of the Oristano Gulf were investigated, considering two different transport timescales: residence time and transit time. Both transport timescales rely on numerical methods. In particular, a Eulerian approach was followed to compute the residence time, whereas a Lagrangian approach was followed to compute the transit time. In this section, the two techniques are described.

2.2.1 Residence time. Residence time is not a well-defined term. In the literature, various meanings are associated with this concept [8–13].

In this work, the residence time was computed through a Eulerian approach and was defined as the time required for each element of the domain to replace most of the mass of a conservative tracer, originally released, with new water. To compute this, we refer to the mathematical expression given by Takeoka [14, 15] known as the remnant function.

The tracer, initially released inside the gulf with a concentration of 100%, is subject to the action of the wind-induced water circulation that drives it out through the inlet. This leads to a decay in its concentration. The remnant function $r(x, y, t)$ of the concentration is given at each position of the domain as $r(x, y, t) = C(x, y, t)/C_0(x, y)$, where $C(x, y, t)$ is the concentration at time t of the passive tracer in the position x, y, and $C_0(x, y) = C(x, y, t = 0)$ is its initial value. The residence time τ can then be defined as [14, 15]:

$$\tau = \int_0^\infty r(t)\,\mathrm{d}t \tag{5}$$

and for every position x, y of the domain as:

$$\tau(x, y) = \int_0^\infty r(x, y, t)\,\mathrm{d}t. \tag{6}$$

If the decay of the concentration C is exponential,

$$C(t) = C_0 \mathrm{e}^{-\alpha t}, \tag{7}$$

then the residence time τ can be computed as $\tau = 1/\alpha$ that is the time it takes to lower the concentration to $1/e$ of its initial value. The residence time was computed for each simulated scenario and for each element of the grid domain.

To compute the spreading and the fate of the tracer, a solute transport model coupled with the hydrodynamic one was used. The model solves the advection and diffusion equation that, in the vertically integrated form, is given as:

$$\frac{\partial C}{\partial t} + \frac{\partial uC}{\partial x} + \frac{\partial vC}{\partial y} = K_{\mathrm{H}} \left(\frac{\partial^2 C}{\partial^2 x} + \frac{\partial^2 C}{\partial^2 y} \right), \tag{8}$$

where C is the solute concentration, u and v are the barotropic velocities, and K_{H} is the horizontal diffusion coefficient. The solute transport model uses the hydrological data produced by the hydrodynamic model to compute the advection and the diffusion of the tracer.

A more complete description of the model may be found in Umgiesser *et al.* [6] and in Cucco and Umgiesser [16].

2.2.2 Transit time. The transit time is generally defined as the time required for a water particle to travel from a location to the boundary of the domain [13–15].

In order to compute the transit time of the Oristano Gulf, a Lagrangian approach was followed. At each model run, the gulf domain is seeded with simulated particles that are transported in the basin and eventually carried out of the domain by the velocity field generated by the hydrodynamic model.

For each particle, the time required to reach the open sea from their initial position is recorded. Then, the transit time for each location of the domain where a particle was released is computed.

In order to compute the fate of the particles within the domain, the Eulerian velocity field produced by the hydrodynamic model was used to advect the particles, and a random walk technique was used to simulate the diffusive processes generated by the small-scale turbulence [9, 17].

The Lagrangian model is coupled with the hydrodynamic model and computes the trajectory followed by each particle with the same time step of the hydrodynamic code. The water levels and the velocity data are used to compute the advection and diffusion of the particles without any further integration in time and in space. Particles within the same element of the numerical grid are advected with the same velocity that is computed by the hydrodynamic model. Otherwise, the trajectories followed by each particle inside the same element are different and depend on the relative position of each particle with respect to the vertices of the element itself.

The particles were released within the basin on a regular distribution in order to fill each element of the finite-element grid with almost one particle. The number of particles required to initialize the model runs was increased, starting from an initial number, until, for the same forcing conditions, the spatial average of the transit time remained constant. Approximately 400,000 labelled particles were released. Each particle is representative of an area of about 400 m^2.

Downloaded At: 12:58 15 January 2011

2.3 *Geochemical analysis*

Within the frame of a study on the biogeochemical characteristics of the Gulf of Oristano [18, 19], the uppermost 5 cm of bottom sediments was collected by scuba divers on a grid of 100 stations using a PVC cores (3 cm internal diameter) in October–December 1997. Several stations located in proximity of the southern part of the basin were selected for the evaluation of spatial differences in sediment-grain-size composition and heavy-metal (Cd, Pb, and Zn) concentration. The selected area is located in the proximity of the Marceddì lagoon inlet, which collects the sewage-treatment-plant discharges from the surrounding cities (Oristano and Cabras) into the gulf.

Before laboratory treatment, the sediments were oven-dried at 40 °C for 1 d; 0.1 g of samples was then treated with hydrogen peroxide (H_2O_2) to eliminate organic material and solubilized in a microwave oven with HNO_3, HCl (1:3), and HF. Particle-size analysis was performed on larger particles by dry sieving with a mesh opening of between −1 and 2.5 and 0.5 spacing. For smaller particles, a laser Galai CIS 1 instrument at analytical size intervals of 0.5 m was used. The concentration of Cd, Pb, and Zn was determined using a Perkin Elmer 3030 Zeeman flameless graphite furnace. The data were interpolated using a Kriging algorithm to obtain the spatial distributions of the heavy-metal concentration in the selected area.

3. General simulation set-up

All simulations presented in this work were carried out using a time step of 100 s. This time step could be achieved due to the unconditionally stable scheme of the finite-element model.

The model was initialized with surface elevations and water currents set to zero. A spin up time of 2 d was used for all the simulations. This time was enough to damp out all the noise

introduced through the initial conditions. The simulations were carried out to reproduce the effect induced by the main wind regimes of the area.

At the open boundary no surface elevation was considered. The water levels were made equal to zero, and the water transports were computed by the model in accordance with a radiative condition. This parameterization was followed to simulate a wind-driven circulation along the closed boundary without generating any water set-up at the open boundaries, which should not be realistic. The number of elements and the distance separating the open boundaries from the interested part of the domain are sufficient to disregard any remarkable influence of the open boundary condition on the numerical results.

In this study, no spatial distinction of the bottom friction was made inside the domain. The Strickler coefficient was considered homogeneous over the whole basin and set equal to $32\,m^{1/3}\,s^{-1}$. The drag coefficient for the momentum transfer of wind was set to 2.5×10^{-3}, which is a default value.

Three different scenarios were investigated: the basin circulation induced by a $10\,m\,s^{-1}$ Mistral wind, $9\,m\,s^{-1}$ Libeccio wind, and $10\,m\,s^{-1}$ Sirocco wind, respectively. The wind intensities correspond to the yearly average values.

The duration of each simulation is about 6 d. The wind intensity reaches its top value after the first 7 h of simulation and then kept constant until the end of the simulation.

The wind forcing is homogeneous in space; no land–sea effect on the wind curl was considered. Even if the numerical application is based on a high-resolution hydrodynamic model, and the spatial scale of the investigated dynamics is lower than 100 m, the effect of the orography on the wind field has not been considered. The adopted parameterization is partially justified by the morphology of the surrounding mainland, which is characterized by the presence of a vast plain, the Campidanese Plain, bordering with the south-eastern perimeter of the gulf, which does not influence either the pattern of the winds blowing from the sea or that from the mainland such as the Sirocco wind.

On the other side, in the southern and northern part of the gulf, the orography is characterized by the presence of the S. Marco and Frasca capes which, being lower than 90 m [1], only slightly control the velocity field patterns of the wind blowing from the sea such as the Mistral and Libeccio wind regimes. Concerning the winds blowing from the mainland such as the Sirocco, the two capes have no influence on the shaping the wind-field patterns in the gulf area. Therefore, even with some degree of uncertainty, the general wind-driven circulation inside the gulf can be reproduced using, as a model-forcing condition, wind data filed constant in space.

Neither tidal nor baroclinic nor other any meteorological forcings were considered in this study; only the wind-driven water circulation was investigated.

4. Results

In this section, the simulation results are presented. The wind-induced water-circulation patterns are described for each forcing scenario. Moreover, the residence time and transit time of the basin are computed and discussed. Finally, the results are compared with geochemical data for the gulf bottom sediment.

4.1 *Mistral wind scenario*

When the model has been forced with a $10\,m\,s^{-1}$ Mistral wind the induced water circulation is mainly governed by an anticyclonic motion. Figure 2 shows a snapshot of the water circulation and water levels 96 h after the beginning of the numerical simulation.

Downloaded At: 12:58 15 January 2011

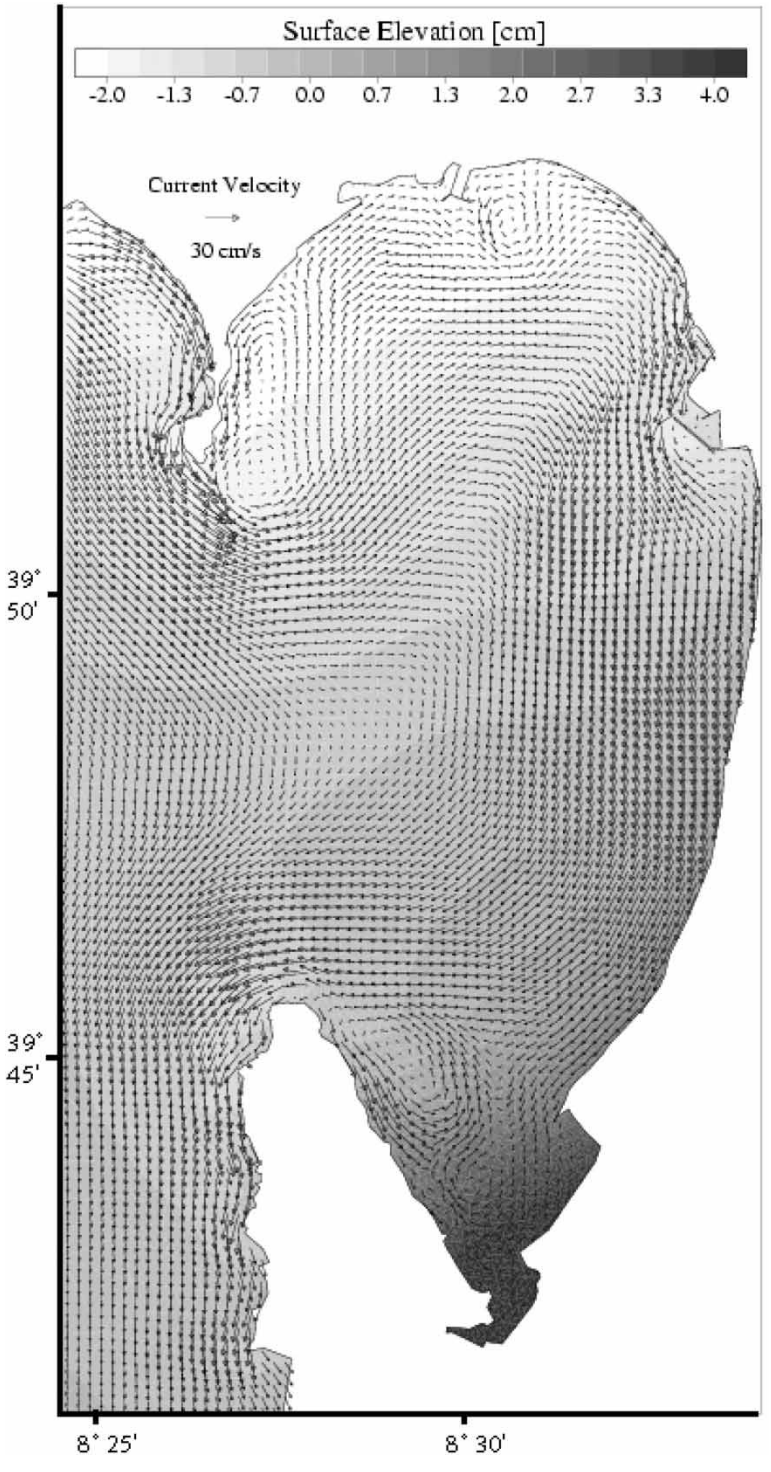

Figure 2. Water current and sea surface elevation in the Gulf of Oristano when the Mistral is forcing the basin. The results were obtained 96 h after the beginning of the simulation.

Downloaded At: 12:58 15 January 2011

The sea water enters the gulf through the inlet, in the nearby San Marco cape (northern cape), fills the basin, and exits around the Frasca cape (southern cape). The water masses follow the main channel of the gulf (see figure 2) toward the north-east, then deviate to the south, generating an intense long-shore stream in the whole central area of the basin. The circulation pattern is characterized by a rotation core located around half the length of the opening, slightly displaced to the mainland side.

After 96 h of simulation, a water-level set-up of about 5 cm is induced by the wind action. The Mistral, pushing the water toward the south-east gulf border, increases the water levels to up to 2 cm in the southern part and decreases the water levels in the northern part of the gulf to values lower than 2 cm (see figure 2).

The computed water fluxes through the inlet are in line with the features of the inner gulf circulation. In figure 3, the intensity of the water transport through the inlets computed after 96 h of simulation is plotted. Water inflow takes place along the northern part of the inlet with a total discharge of about 10,560 $m^3\ s^{-1}$, whereas the water outflow occurs along the southern part of the inlet with a total discharge of about 10,790 $m^3\ s^{-1}$ (see table 1).

The maximum current velocities are detected in the northern part of the inlet in the proximity of the San Marco cape, where values higher than 40 cm s^{-1} are reached. Similar current speed values are found in the inner part of the basin near the eastern border. An intensification of the current is also detected in the proximity of the Frasca cape. In this area, the maximum current speed is about 35 cm s^{-1}.

Along the borders of the gulf, in the proximity of the two capes and the coastline irregularities, such as the two harbours, the water circulation is characterized by the presence of vortices. In particular, off the lee side of the San Marco cape (see figure 2), a large cyclonic vortex is generated by the wind action and the inertial components of the water circulation. This area is characterized by low current velocities (lower than 5 cm s^{-1}) and can be characterized by strong trapping phenomena.

Downloaded At: 12:58 15 January 2011

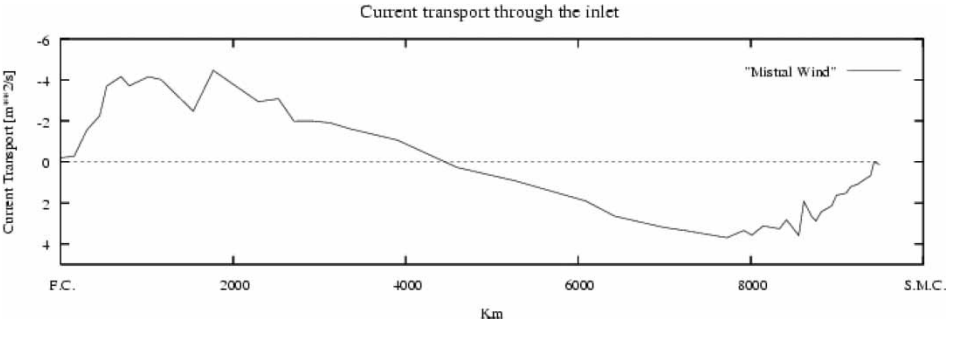

Figure 3. Water transport through the inlet, Mistral wind scenario. Units on the y-axis are m^2/s.

Table 1. Inflow and outflow ($m^3\ s^{-1}$) through the inlet for the three simulated scenarios (I) Mistral wind forcing, (II) Libeccio wind forcing, and (III) Sirocco wind scenario.

Discharge	I	II	III
Inflow	10 561	8785	7469
Outflow	10 790	8519	7171

Smaller cyclonic structures are also detected in the vicinity of the touristic and industrial harbours. The vortices are located on the lee side of the harbour dikes where the current velocity is reduced to values of 2–3 cm s^{-1}.

In the southern part of the gulf, surrounding the Frasca cape (see figure 2), a one pair vortex system is generated by the wind action and the inertial components of the current field. A large cyclonic gyre is detected in the proximity of the cape, whereas a smaller anticyclonic gyre is generated in the vicinity of the Marceddi lagoon inlet. These circulation patterns tend to trap the water in this area, isolating it from the main circulation of the gulf. In the core of the vortices, the current velocity is weak (values lower than 10 cm s^{-1}), whereas a stronger stream (values greater than 35 cm s^{-1}) is generated between them.

This area is in front of the inlet of a lagoon system (the Marceddi lagoon) that collects discharges from many different anthropic activities. Therefore, this area can be classified as a possible risk zone for pollutant accumulation due to both the presence of anthropic inputs and the features of the circulation pattern.

From the transport timescale computation, the average values of the residence time and transit time for the basin are about 1.2 ± 0.8 and 1.4 ± 1.7 d, respectively (see table 2). Both residence and transit times are characterized by low average values, which reveal the high cleaning efficiency of the water circulation when the Mistral wind is forcing the basin. The coefficient of variation computed from the statistics is 66% for the residence time and 120% for the transit time. The distribution of both transport timescales is characterized by a high spatial variability, which can be explained by the intensity of the Mistral-wind-induced water circulation that drives the tracer out of the basin almost homogeneously.

In figures 4 and 5, the spatial distributions of the residence and transit time are reported. From a qualitative analysis, the maps present an inverse correlation between the two transport timescale distributions. The water-residence time values increase from the northern to the southern part of the gulf, whereas the transit-time values increase from south to north. This can be explained, taking into account the differences between the concepts of the two transport timescales considered.

In particular, the water-residence time, being an estimate of the time required for each element of the domain to be flushed, presents low values in the northern part of the gulf, where the tracer is quickly flushed by the sea water entering through the inlet. On the other hand, it presents higher values in the southern part of the basin where all the tracer released in the northern part is forced to pass through.

Concerning the transit time, being defined as the time required for each water particle to exit from the basin, this shows lower values in the southern part of the gulf where the particles initially released are quickly carried out of the domain by the water outflow. On the other hand, higher transit-time values are detected in the northern part of the basin where the particles initially released, before flowing out of the gulf through the southern part of the inlet, are carried along the whole domain from the water circulation.

In both maps (figures 4 and 5), areas where the water circulation is characterized by the vortex patterns show high values for the transport timescales. In particular, both the residence

Table 2. Average values of residence and transport times for the three simulated scenarios (I) Mistral wind forcing, (II) Libeccio wind forcing, and (III) Sirocco wind scenario.

Transport time scale	I	II	III
Residence time (d)	1.2 ± 0.8	1.5 ± 1.2	1.9 ± 1.4
Transit time (d)	1.4 ± 1.7	1.4 ± 1.4	1.5 ± 1.4

Downloaded At: 12:58 15 January 2011

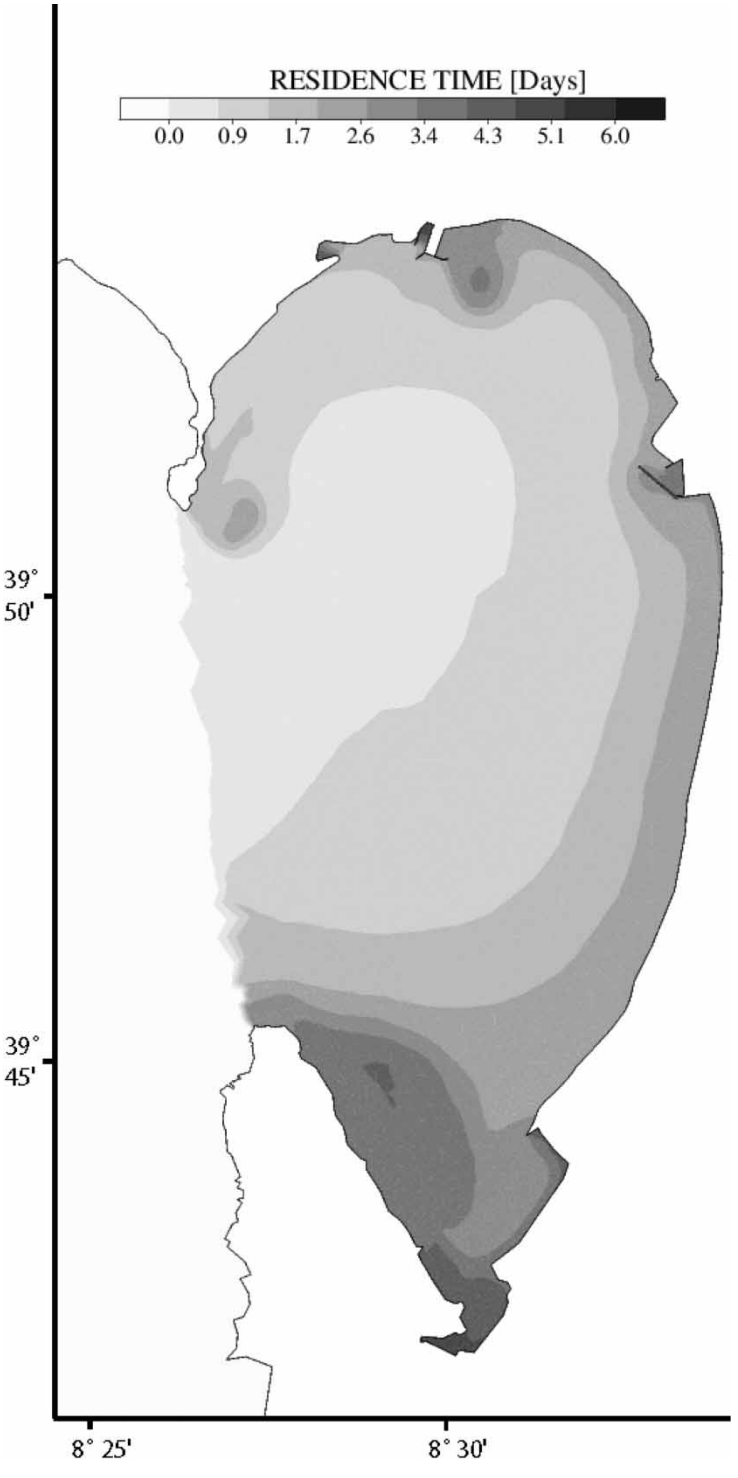

Figure 4. Water-residence-time distribution in the Oristano Gulf, Mistral wind scenario.

Downloaded At: 12:58 15 January 2011

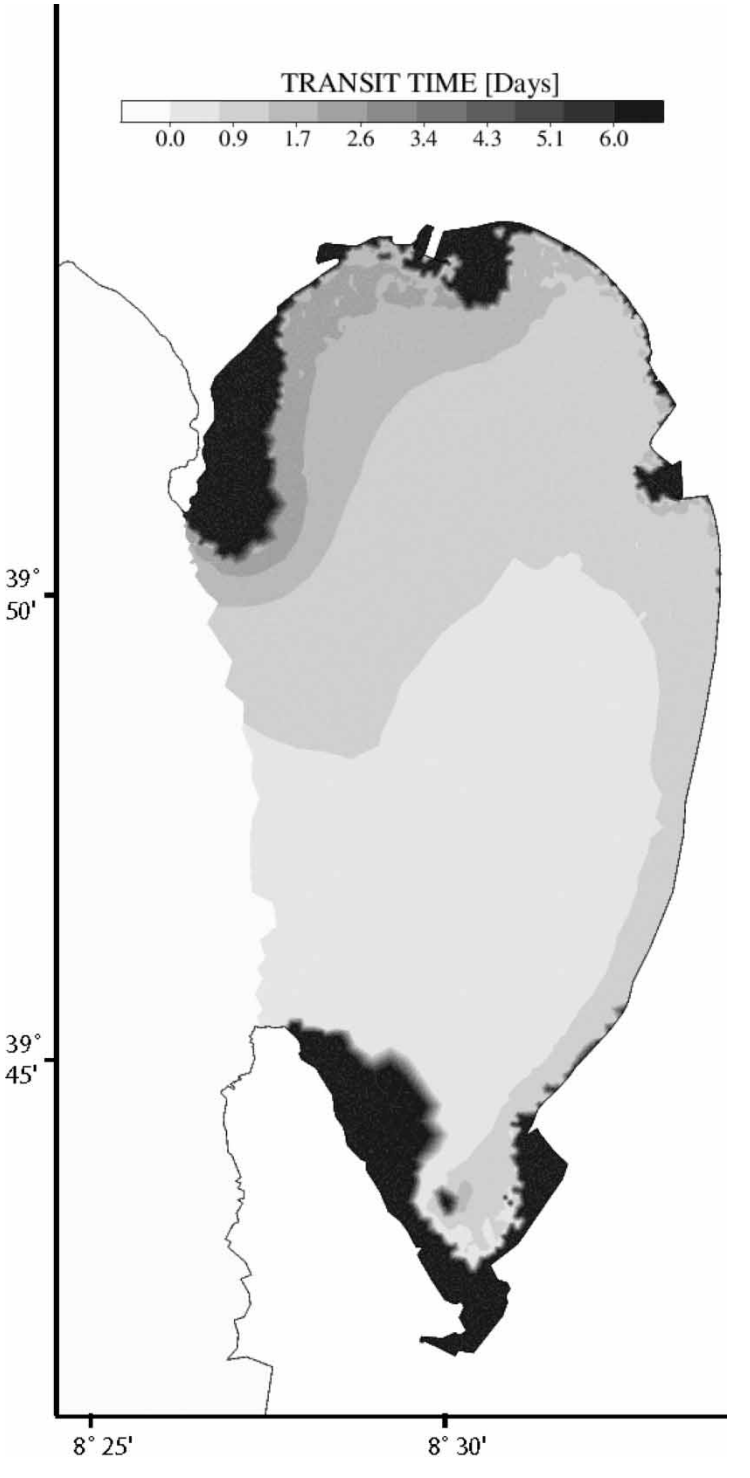

Figure 5. Water-transit-time distribution in the Oristano Gulf, Mistral wind scenario.

Downloaded At: 12:58 15 January 2011

time and the transit time show high values in the south side of the San Marco cape, in the north side of the Frasca cape, and in the lee side of the main harbour dikes. In these areas, characterized by both a low current velocity and a low renewal capacity, the dissolved tracer and the dispersed particles are trapped.

4.2 *Libeccio wind scenario*

When the Libeccio wind is forcing the water currents, the water circulation is radically changed with respect to the previous case. Figure 6 shows a map of the water circulation and water levels computed by the model after 96 h of simulation. The Libeccio-wind-induced circulation is mainly governed by a cyclonic motion. The sea water enters the gulf through the opening, in the vicinity of the Frasca cape (southern part), and exits around the San Marco cape (northern part). The rotation core of the cyclonic motion is located close to the northern cape along the line connecting the two capes. The water-level set-up is reduced with respect to the Mistral wind case, and a water level set-up of about 3 cm is measured along the gulf major axis.

Figure 7 shows the intensity of the water transport through the inlets after 96 h from the beginning of the simulation. The water inflow and outflow through the inlet are decreased with respect to the Mistral wind case. The total amount of water entering in the gulf is about $8780\,m^3\,s^{-1}$, whereas the total amount of water exiting from the gulf is about $8510\,m^3\,s^{-1}$ (see table 1).

Even if the wind speed is slightly lower than in the previous case, the induced water circulation is strongly reduced. This is due to the direction of the Libeccio wind that promotes a lower exchange with the open sea with respect to the Mistral wind case.

The maximum current velocities are detected in the proximity of the San Marco cape (northern part), where values higher than $45\,cm\,s^{-1}$ are reached. The water in this area flows along the main gulf channel toward the open sea. High current speed values are detected along this channel. As for the previous case, similar current speed values (about $40\,cm\,s^{-1}$) are found in the inner part of the basin near the eastern gulf border. The Frasca cape area is characterized by a slight intensification of the water current. In this area, the maximum current speed is about $20\,cm\,s^{-1}$.

In this case, a large anticyclonic vortex is detected in the northern part of the basin. The vortex length embraces the whole area located at north of the main gulf channel between the San Marco cape and the touristic harbour. The inner part of this area corresponds to the rotation core of the anticyclonic motion and is characterized by low values of current velocity. On the other hand, along the edges of the vortex, high current speeds are detected.

As for the Mistral wind scenario, the Libeccio wind action generates a vortex system in the southern part of the gulf (see figure 6). Nevertheless, contrary to the previous case, the larger eddy located in the proximity of the Frasca cape is governed by an anticyclonic motion, whereas the smaller one, in the nearby Marceddi lagoon inlet, is characterized by a cyclonic motion. Also, in this case, the two vortices present a core of rotation where the current velocity is very weak, and the water with its suspended or dissolved load can be trapped.

From the basin-transport-timescale analysis, the average values for residence time and transit time are 1.5 ± 1.2 and 1.4 ± 1.4 d, respectively (see table 2). The basin flushing efficiency when the Libeccio wind is forcing the water circulation, is comparable with that obtained in the Mistral wind case. In fact, similar results with respect to the previous scenario were obtained for both the residence time and the transit time. The coefficient of variation of the two distributions is still high, about 80% and 100% for the residence time and transit time, respectively. The results reveal also that the Libeccio wind promotes a heterogeneous flushing of the basin.

Downloaded At: 12:58 15 January 2011

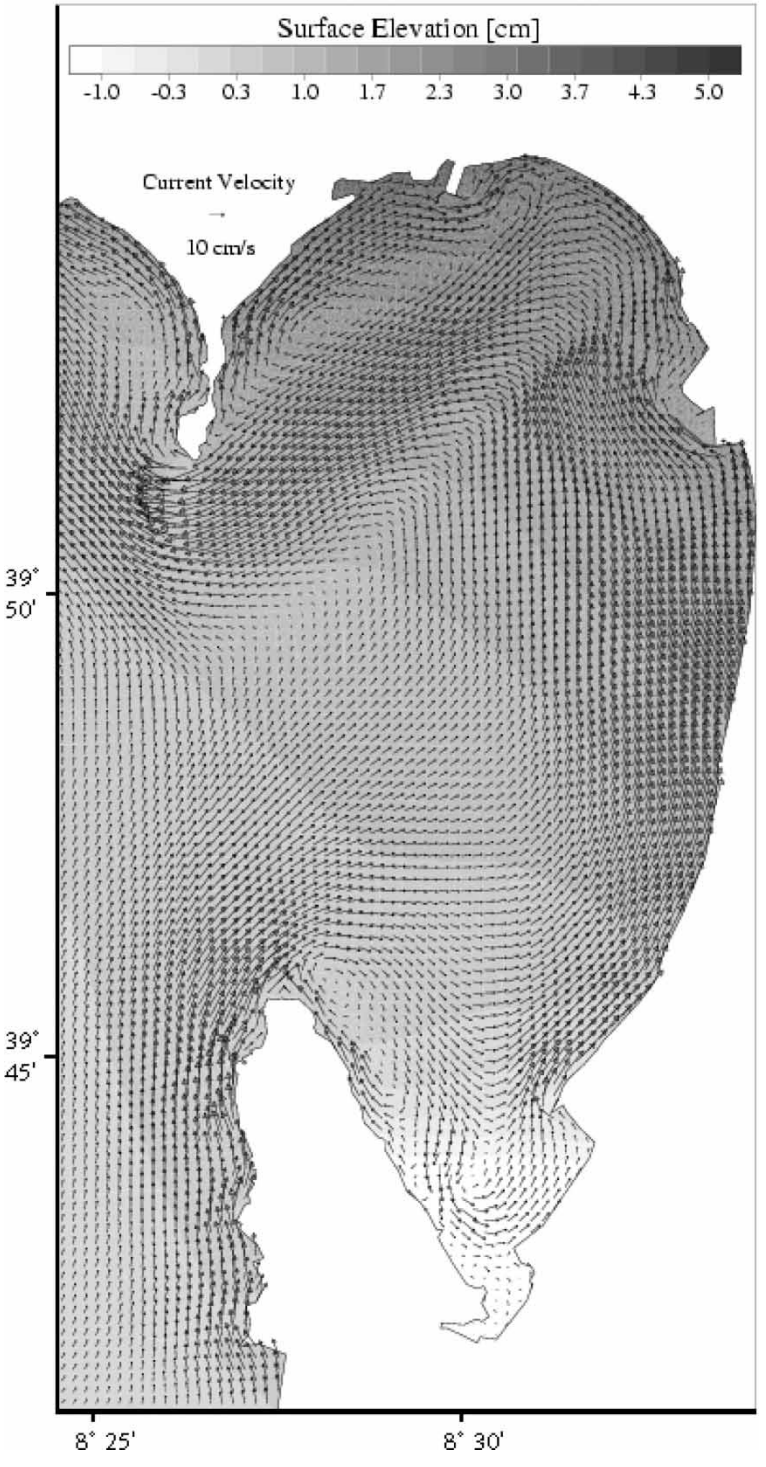

Figure 6. Water current and sea surface elevation in the Gulf of Oristano when, Mistral wind scenario. The results were obtained 96 h after the beginning of the simulation.

Downloaded At: 12:58 15 January 2011

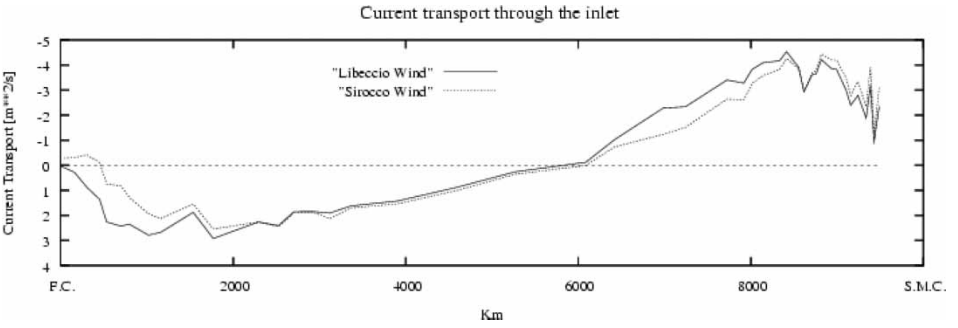

Figure 7. Water transport through the inlet, Sirocco and Libeccio wind scenario. Units on the y-axis are m^2/s.

Figures 8 and 9 show the residence time and the transit time spatial distributions. Also, in this case, for the central areas of the gulf, the residence-time and transit-time distributions show an inverse correlation. Nevertheless, in this case, higher residence-time values are detected in the northern part, whereas lower values are found in the southern areas. On the other hand, lower transit-time values are found in the northern areas, and higher values are found in the southern areas.

Two main areas, corresponding to the large northern anticyclonic vortex and to the southern cyclonic vortex, show high values of both residence and transit time. As for the previous case, the wind action and the coastline irregularities generate such circulation patterns characterized by a low current velocity and weak renewal efficiency, promoting possible trapping phenomena.

Downloaded At: 12:58 15 January 2011

4.3 *Sirocco wind scenario*

In the Sirocco wind scenario, the basin-water circulation is dominated by a cyclonic motion (see figure 10). The sea-water masses enter the basin through the southern part of the opening in the nearby Frasca cape, and flow out of the gulf through the northern part of the opening, close to San Marco cape, after being transported inside the basin. The rotation core of the cyclonic motion is situated in the vicinity of the northern cape along the line connecting the two capes. No intense water-level set-up is generated by Sirocco wind forcing, and a value lower than 3 cm is computed by the model.

In figure 7, the water transports through the opening are reported 96 h after the beginning of the simulations. The shape of the water-transport distribution is similar to that obtained from the Libeccio wind case; nevertheless, in this case, the intensities of the water inflow and outflow are decreased. The total amount of water entering the gulf is about $7469\,m^3\,s^{-1}$, whereas water exiting from the gulf is about $7171\,m^3\,s^{-1}$ (see table 1). Even if the intensity of the Sirocco wind is higher than the Libeccio wind case, the water fluxes through the opening are lower. The sirocco wind is unable to promote intense exchange with the open sea.

As for the Libeccio scenario, high current speed values are detected in the northern part of the inlet in the nearby San Marco cape. In this area, the current velocity reaches maximum values of $45\,cm\,s^{-1}$. In the northern part of the basin, the Sirocco wind forces the water circulation to follow the gulf coastline. High current speeds are detected along the northern edge of the main gulf channel (maximum current velocity of about $38\,cm\,s^{-1}$) and along the eastern gulf coast (maximum current velocity of about $40\,cm\,s^{-1}$). Also, for this forcing scenario, the southern part of the gulf is characterized by an intensification of the current

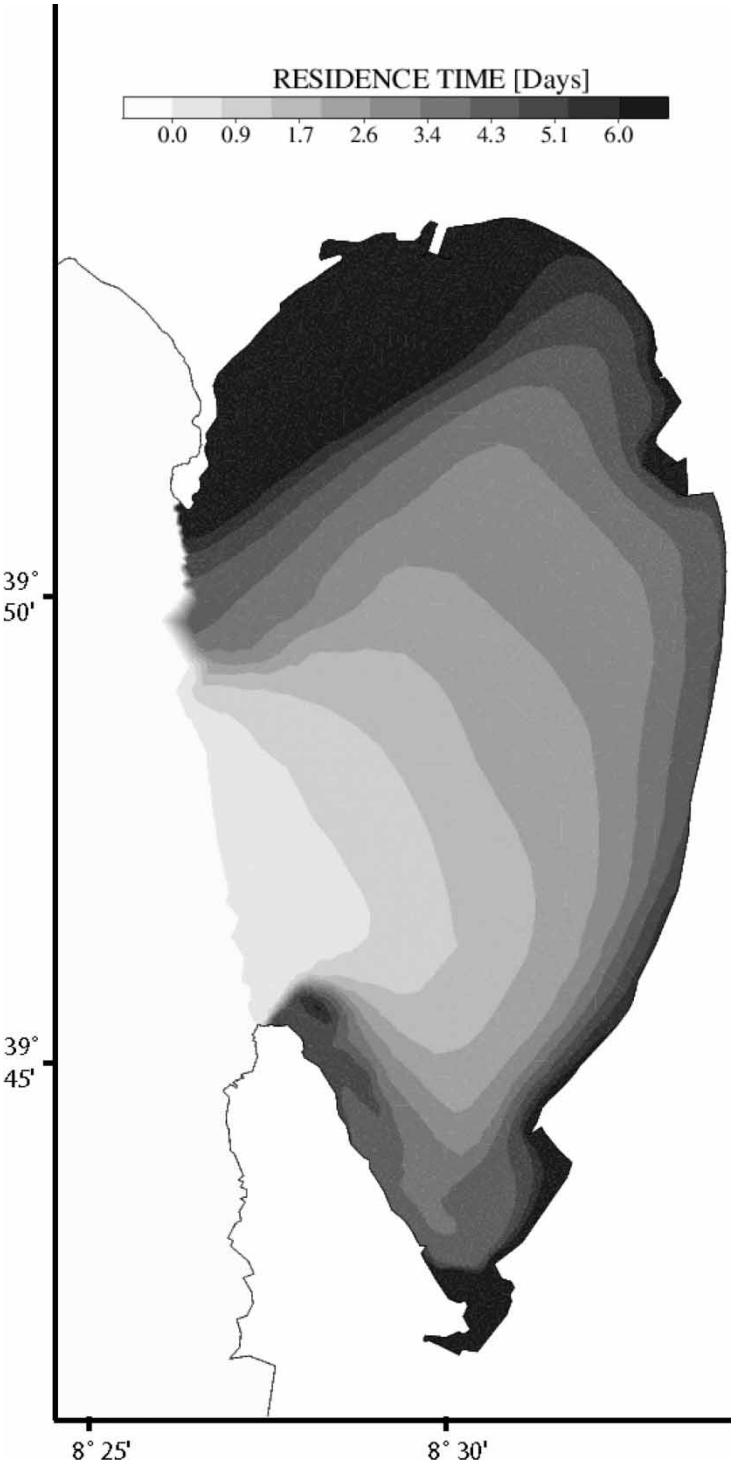

Figure 8. Water-residence-time distribution in the Oristano Gulf, Mistral wind scenario.

Downloaded At: 12:58 15 January 2011

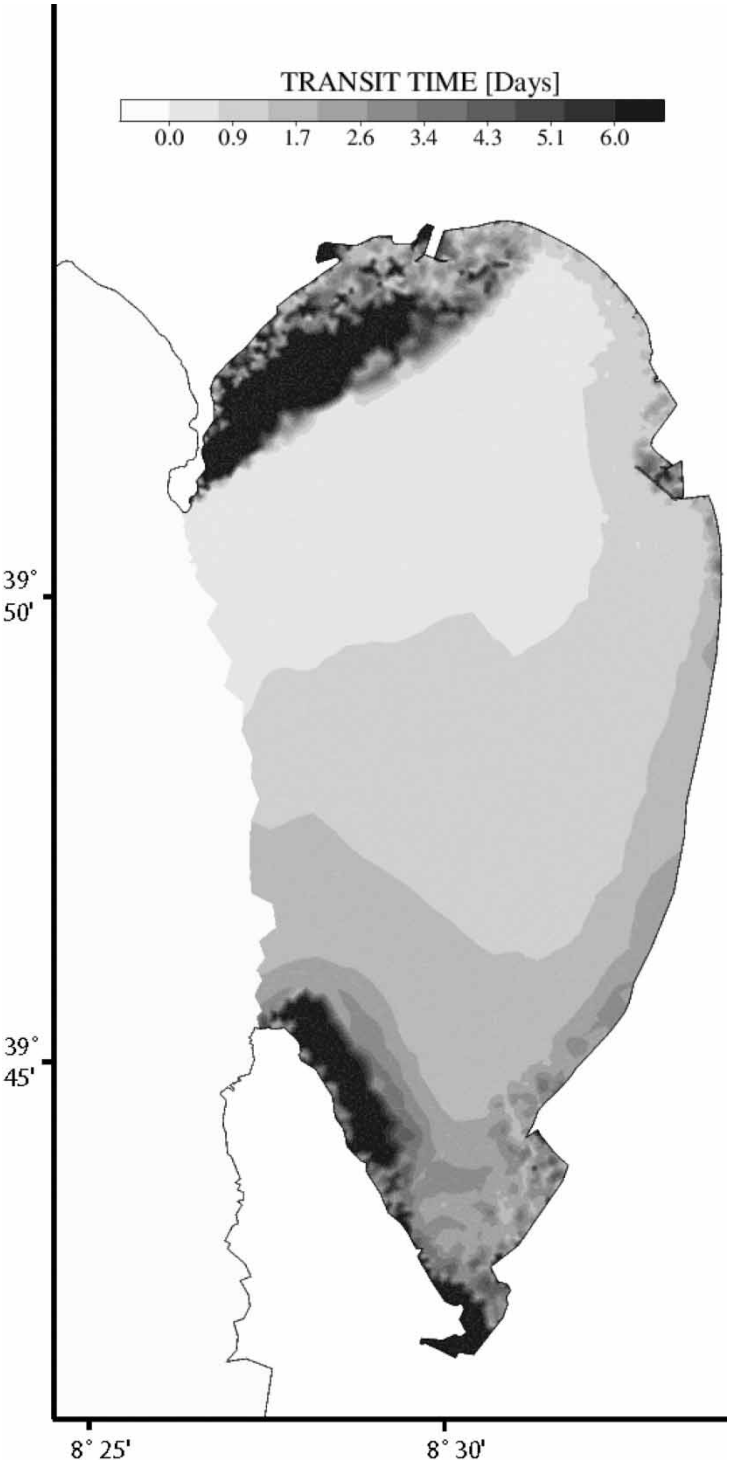

Figure 9. Water-transit-time distribution in the Oristano Gulf, Mistral wind scenario.

Downloaded At: 12:58 15 January 2011

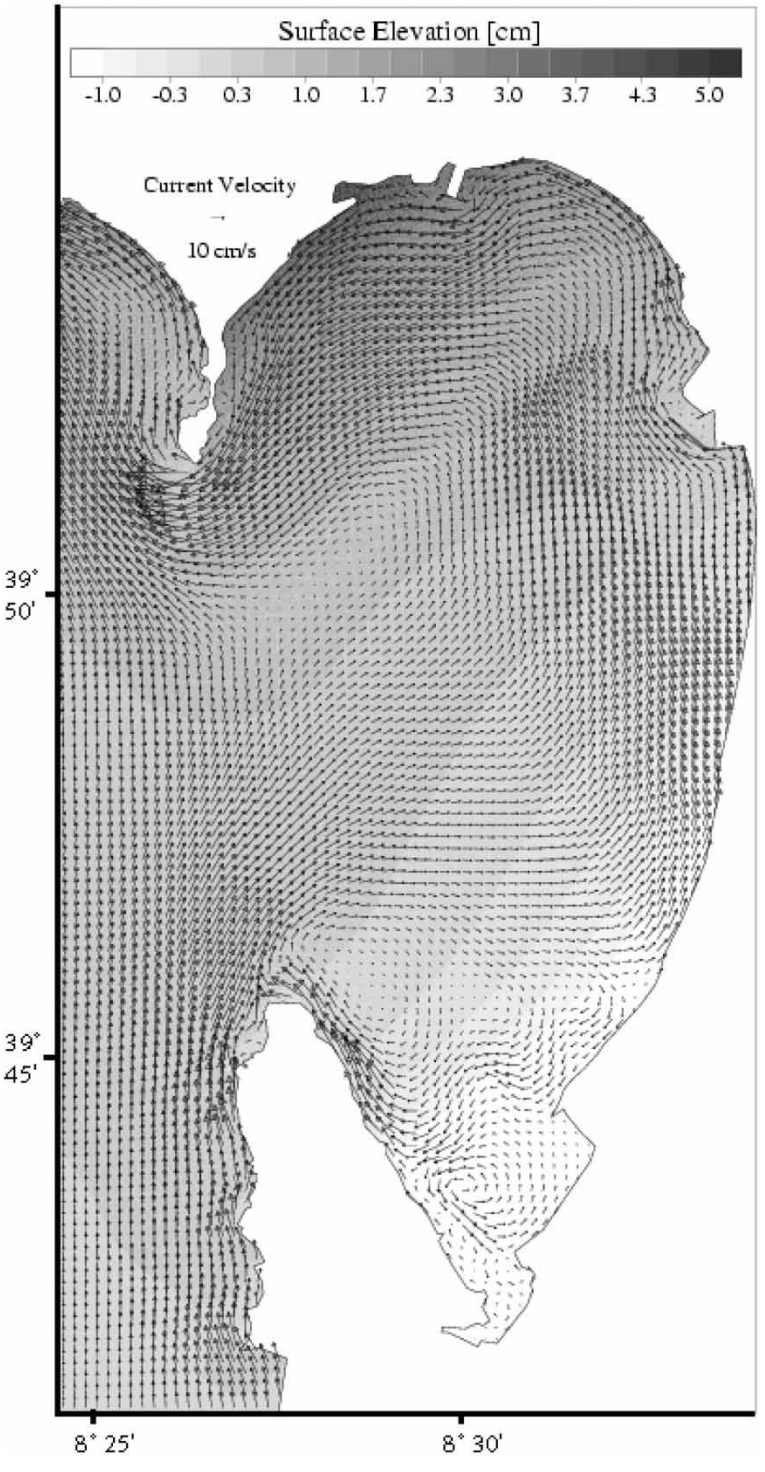

Figure 10. Water current and sea surface elevation in the Gulf of Oristano, Mistral wind scenario. The results were obtained 96 h after the beginning of the simulation.

Downloaded At: 12:58 15 January 2011

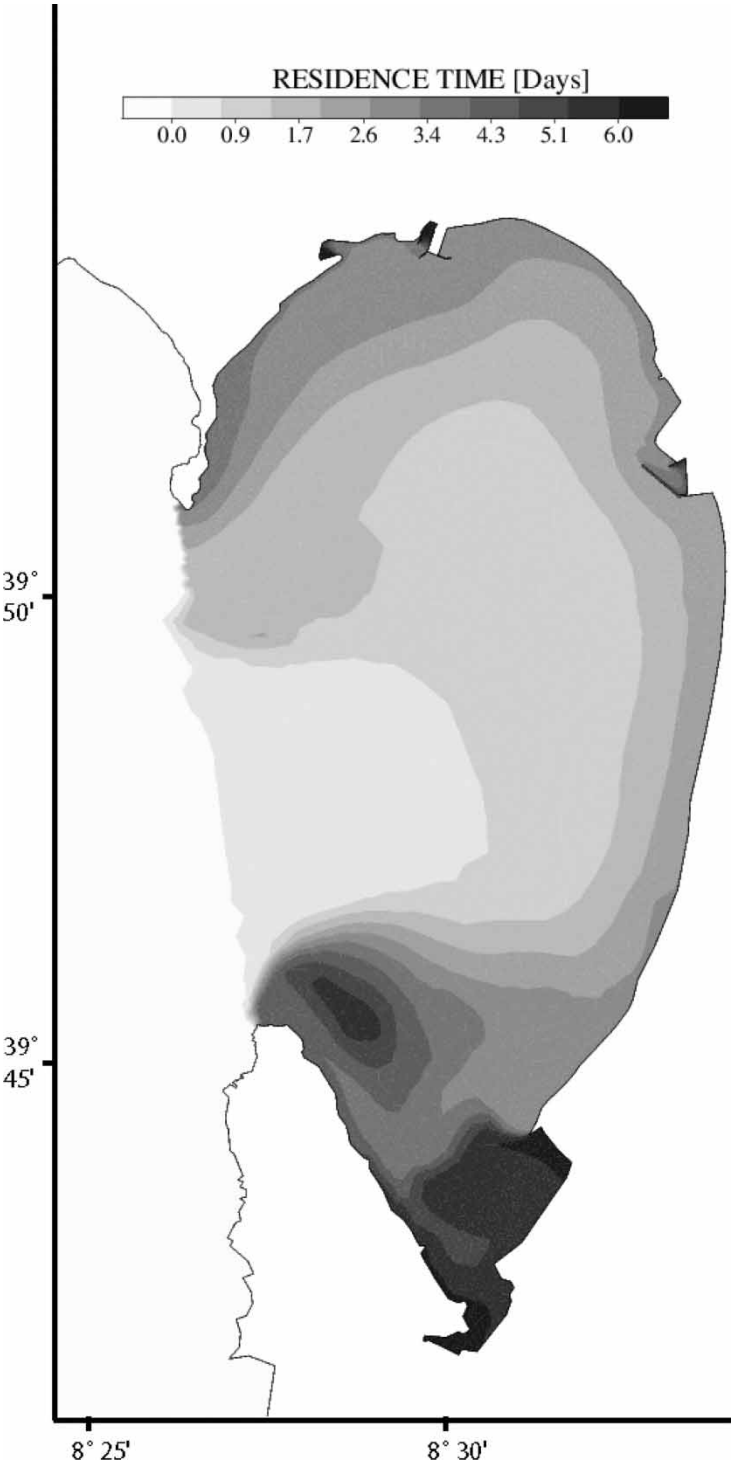

Figure 11. Water-residence-time distribution in the Oristano Gulf, Mistral wind scenario.

Downloaded At: 12:58 15 January 2011

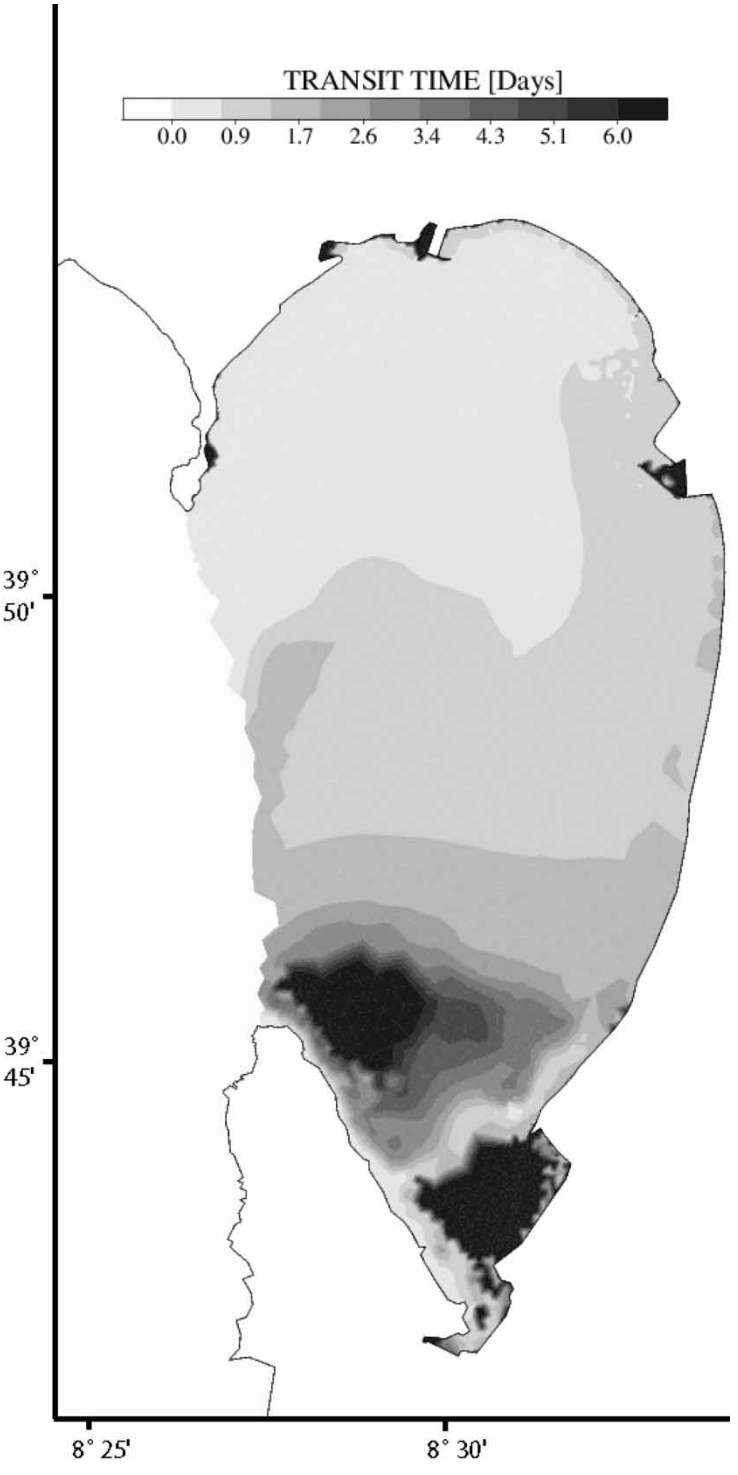

Figure 12. Water-transit-time distribution in the Oristano Gulf, Mistral wind scenario.

Downloaded At: 12:58 15 January 2011

velocity in the proximity of the Frasca cape. In this area, the inflow current can reach values of about 35 cm s^{-1}.

The Sirocco wind, in contrast to the previous two cases, is unable to generate any considerable vortex system in the northern part of the gulf. In this area, the water flows out of the basin following the coastline and the bathymetry without being trapped by any local circulation pattern.

On the other hand, the Sirocco wind generates a pair of vortices in the southern part of the gulf. A large anticyclonic vortex is located along the northern side of the Frasca cape, and a small cyclonic vortex is located in front of the Mistras lagoon inlet. The anticyclonic motion covers a vast area between the Frasca cape and the eastern boundary of gulf. The current velocity is high in the area between the two vortices where an intense easterly stream is generated (see figure 10). On the other hand, low values of the current speeds are detected in the core of the two vortices where trapping phenomena can be promoted.

The residence and the transit time were computed also for this forcing scenario. From the statistics (see table 2), the basin average residence time and transit time are 1.9 ± 1.4 and 1.5 ± 1.4 d, respectively. With respect to the previous two cases, the residence and the transit time show the highest values. The Sirocco wind action reduces the cleaning capacity of the basin with respect to the previous two cases. The computed coefficients of variation for the two distributions are 73% for the residence time and 93% for the transit time. These results still reveal a high variability in transport timescales over the domain.

Figures 11 and 12 show the spatial distribution of the residence time and transit time. Also, in this case, the inverse correlation between the two distributions can be observed for the central areas of the gulf: the higher the residence time values, the lower the transit time values, and vice versa.

In this case, in the northern part of the gulf, there is no evidence of trapping phenomena. No areas characterized by both high residence and transit time values can be detected. This is due to the wind action that prevents the generation of any vortex system in the northern part of the basin. On the other hand, in the southern part of the gulf, where the wind action generates a vortex system, both the residence time and the transit time show high values. As for the previous cases, strong trapping phenomena can be promoted in areas where the vortices are generated.

Downloaded At: 12:58 15 January 2011

5. Discussion

To compare model results with field measurements, the residence-time and the transit-time spatial distribution obtained for each forcing scenario were compared with empirical data for heavy-metal distribution inside the gulf.

The basic hypothesis is that areas characterized by high values of both residence and transit times are subject to strong trapping phenomena. In these areas, the circulation pattern is characterized by the presence of vortex structures that prevent the water masses initially released from exiting quickly. Therefore, the suspended load carried by the currents should be subject to sinking and deposition processes. Consequently, in these areas, the geochemical features of the sediment should be distinguishable from the overall basin.

Figures 13–15 show the distribution of Cd, Zn, and Pb concentrations in the sediments [19]. The data were interpolated to obtain the spatial distributions of heavy-metal concentrations in the selected area.

The gradient of the concentration is not homogeneous, as we expected, if the transport process was mainly driven by the diffusion phenomena. On the contrary, the concentration

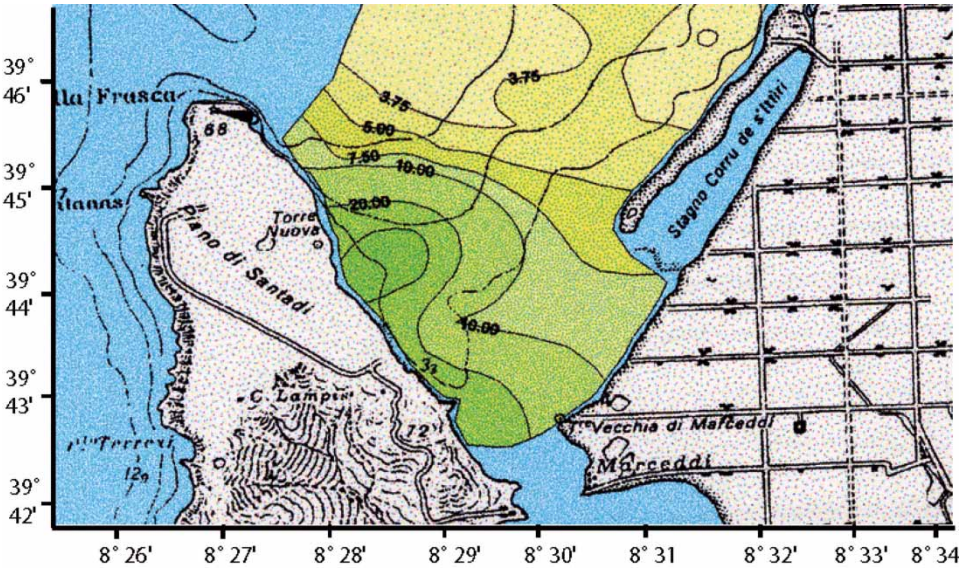

Figure 13. Cd concentration in the bottom sediment of the southern part of the gulf. The units are mg kg^{-1}.

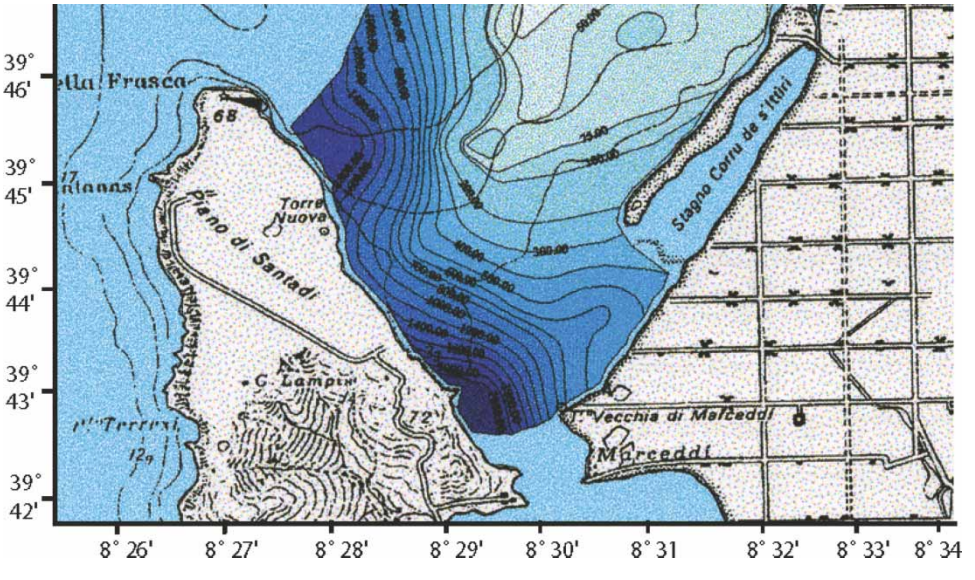

Figure 14. Zn concentration in the bottom sediment of the southern part of the gulf. The units are mg kg^{-1}.

values in all cases show two local maxima, the first corresponding to the Marceddi lagoon inlet, on the eastern gulf border, and the second, characterized by higher values, located approximately in front of the northern side of the Frasca cape. The spatial pattern of Pb concentration differs slightly from those of Cd and Zn; this is probably due to a local anomaly in the Pb concentration evidenced by the interpolation process. Nevertheless, the general trend of Pb concentration in the area is similar to that of the Cd and Zn concentrations.

Downloaded At: 12:58 15 January 2011

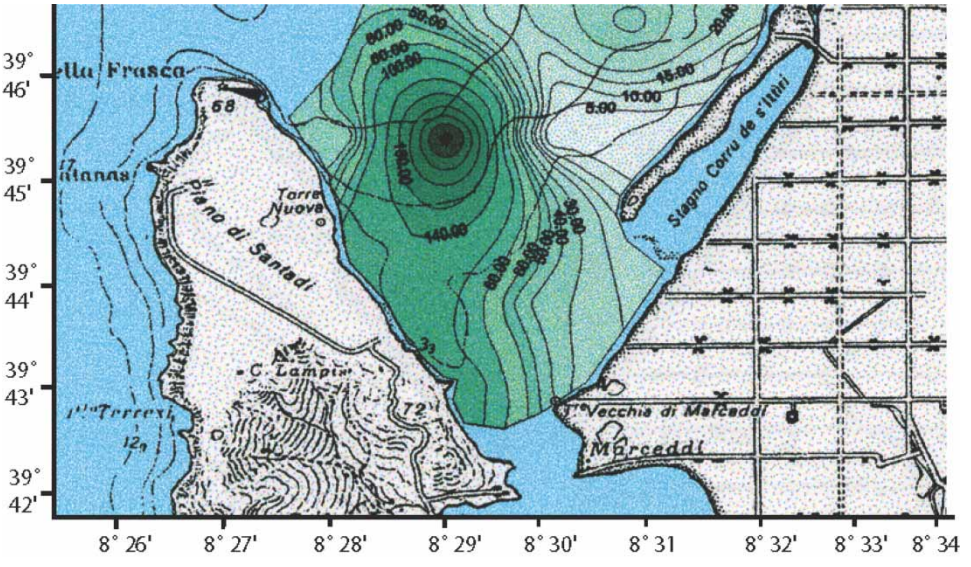

Figure 15. Pb concentration in the bottom sediment of the southern part of the gulf. The units are mg kg^{-1}.

Downloaded At: 12:58 15 January 2011

Considering that the possible source of suspended heavy-metal particles is the adjacent Marceddi lagoon system, the two local maxima can be explained by taking into account both the circulation patterns and the transport timescale distribution in the area. In particular, from the hydrodynamic results, the southern part of the basin is characterized by the presence of a one-pair vortex system promoting strong trapping phenomena.

From the comparison of the two transport timescale results (figures 2, 5, and 8) with the geochemical results (see figures 11–13), it is evident that the maximum values of the heavy-metal concentration in the sediment are detected in areas where the circulation is dominated by vortex dynamics, and the trapping process is promoted. In these areas, the dispersed heavy-metal loads are subject to sinking processes and can be accumulated by the sediments.

Therefore, a preliminary model validation was carried out. In fact, the circulation pattern in the southern part of the basin, as described by the hydrodynamic model, partially matches the sedimentological features of the area.

6. Conclusions

In this work, the circulation of the Oristano Gulf was investigated by means of a 2D hydrodynamic model. The model is based on the finite-element method. This numerical method is the most suitable solution to reproduce the complex geometry of the basin.

The study was carried out considering the wind as the main process influencing the water circulation of the basin. Neither the tide nor the freshwater input nor the large-scale offshore circulation was taken into account.

Three different forcing scenarios were reproduced: the water circulation induced by a 10 m s^{-1} Mistral wind (NW), by a 9 m s^{-1} Libeccio wind (SW), and by a 10 m s^{-1} Sirocco wind (SE). The wind intensities correspond to the yearly average values.

For each forcing scenario, the water circulation and the transport timescales were investigated. In particular, both the basin residence time and transit time were computed for each simulation.

In the Mistral wind scenario, the general circulation is dominated by an anticyclonic motion. On the other hand, because of the different direction, both the Libeccio and the Sirocco wind action generate cyclonic motion of the water inside the basin.

The basin renewal efficiency is generally high under each forcing condition. The residence time and transit time show similar results for all scenarios. Under the Mistral wind forcing, 1.5 d is required to renew the 70% of the gulf water. Similar values are found for the Libeccio and Sirocco wind scenarios.

Around the two capes of the gulf and in the vicinity of the coastline irregularities, such as the gulf harbours, the wind action generates circulation patterns characterized by vortice systems.

In particular, in the southern part of the basin, for each forcing situation, a vortex system is generated. In the Mistral wind forcing scenario, a large cyclonic vortex is detected along the northern side of the Frasca cape (the southern cape), and a smaller anticyclonic vortex is generated in front of a lagoon system (the Marceddi lagoon). On the other hand, both Libeccio and Sirocco winds generate a large anticyclonic vortex along the northern side of the Frasca cape and a smaller anticyclonic vortex in front of the Marceddi lagoon inlet.

In the northern part of the gulf, around the San Marco cape (the northern cape), the Mistral wind and Libeccio wind generate a small cyclonic vortex and large anticyclonic vortex, respectively. On the other hand, in this area, no vortex system is generated by the Sirocco wind action.

In areas characterized by the presence of vortices, both the water residence time and transit time show high values, revealing a weak renewal efficiency. Strong trapping phenomena can be promoted in these areas where the current velocity is low.

These preliminary results are partially confirmed by the heavy-metal distribution. In particular, in the Frasca cape area, high heavy-metal concentrations are detected in the bottom sediment of areas where the model results reveal a strong trapping capacity. These zones correspond to the cores of the two vortices generated by the wind action, where the low current speed values and the circulation pattern promote the sinking of dispersed loads in the water.

The water circulation inside the gulf, as described by the model, was partially confirmed by experimental observations. In the southern part of the basin, the hydrodynamic patterns induced by the action of the main winds are partially correlated to the heavy-metal distribution in the sediment.

This work is a first attempt to apply a high-resolution hydrodynamic numerical model to study the wind-driven circulation in the Oristano Gulf. The results obtained, even if only partially confirmed by the experimental data, reveal the possible features and locations of the main circulation patterns induced by the wind scenarios. Furthermore, this application can be considered a useful preliminary investigation to plan future measurement campaigns to investigate and resolve small-scale circulation patterns that characterize the Oristano Gulf.

A conclusive remark intends to stress the promising potential of the followed methodology, which consists in the intercomparison between hydrodynamic features and sedimentological features both to validate the hydrodynamic model results and to explain the variability of the empirical data.

Downloaded At: 12:58 15 January 2011

Acknowledgements

The authors wish to thank Prof. Massimiliano Di Bitetto, for his suggestions and the support offered.

References

[1] M. Pinna. The climate. In *The Oristano Province: The Territory, the Nature and the Men* (in Italian), Provincia di Oristano (Ed.), pp. 38–48, Pizzi Spa, Milan (1989).

[2] C. Ferrarin, G. Umgiesser. Hydrodynamic modeling of a coastal lagoon: The Cabras lagoon in Sardinia, Italy. *Ecol. Model*., **188**, 340–357 (2005).

[3] G.D. Falco. Personal communication (2006).

[4] G. Umgiesser, A. Bergamasco. A staggered grid finite element model of the Venice Lagoon. In *Finite Elements in Fluids*, K. Morgan, E. Ofiate, J. Periaux, O.C. Zienkiewicz (Eds), pp. 659–668, Pineridge Press, Swansea, UK (1993).

[5] G. Umgiesser, A. Bergamasco. Outline of a primitive equation finite element model. In *Rapporto e Studi*, Vol. XII, pp. 291–320, Istituto Veneto di Scienze, Lettere ed Arti, Venice (1995).

[6] G. Umgiesser, D.M. Canu, A. Cucco, C. Solidoro. A finite element model for the Venice Lagoon. Development, set up, calibration and validation. *J. Mar. Syst*., **51**, 123–145 (2004).

[7] A. Cucco, G. Umgiesser. Modeling water exchanges between the Venice Lagoon and the Adriatic Sea. In *Scientific Research and Safeguarding of Venice, Research Program 2000–2004. Results*, P. Campostrini (Ed.), Vol. 3, Multigraf Venice (2005).

[8] B. Bolin, H. Rodhe. A note on the concepts of age distribution and transit time in natural reservoirs. *Tellus*, **25**, 58–63 (1973).

[9] J.T.F. Zimmerman. Mixing and flushing of tidal embayments in the Western Dutch Wadden Sea, Part 1: Distribution of salinity and calculation of mixing time scales. *Neth. J. Sea Res*., **10**, 149–191 (1976).

[10] J. Dronkers, J.T.F. Zimmerman. Some principles of mixing in tidal lagoons, paper presented at Oceanologica Acta Proceedings of the International Symposium on Coastal Lagoons, Bordeaux, France, 9–14 September, 1981, pp. 107–117 (1982).

[11] J.V. de Kreeke. Residence time: application to small boat basins. *J. Waterw. Port Coast. Ocean Eng. ASCE*, **109**, 416–428 (1983).

[12] D. Prandle. A modeling study of the mixing of 137 cs in the sea of the european continental shelf. *Phil. Trans. R. Soc. Lond*., **310**, 407–436 (1984).

[13] C. Wang, M. Hsu, A. Kuo. Residence time of the danshueiiver estuary, Taiwan. *Estuar. Coast. Shelf Sci*., **60**, 381–393 (2004).

[14] H. Takeoka. Exchange and transport time scales in the Seto Inland Sea. *Cont. Shelf Res.*, **3**, 327–341 (1984).

[15] H. Takeoka. Fundamental concepts of exchange and transport time scales in a coastal sea. *Cont. Shelf Res*., **3**, 311–326 (1984).

[16] A. Cucco, G. Umgiesser. Modeling the Venice Lagoon water residence time. *Ecol. Model*., **193**, 123–145 (2005).

[17] H. Ridderinkhof, J.T.F. Zimmerman. Chaotic stirring in a tidal system. *Science*, **258**, 1107–1111 (1992).

[18] G. Cancemi, M. Baroli, G.D. Falco, S. Agostani, G. Piergallini, I. Guala. Integrated mapping of superficial marine meadows as indicators of human impact on coastal zones. *Biol. Mar. Mediterr*., 7 (2000).

[19] G.D. Falco, S. Ferrari, G. Cancemi, M. Baroli. Relationships between sediment distribution and posidonia oceanica seagrass. *Geo. Mar. Lett*., **20**, 50–57 (2000).

Downloaded At: 12:58 15 January 2011